

TA7
W342.R5
V.8
no.3

US-CE-C Property of the
United States Government

The REMR Bulletin

News from the Repair, Evaluation, Maintenance,
and Rehabilitation Research Program

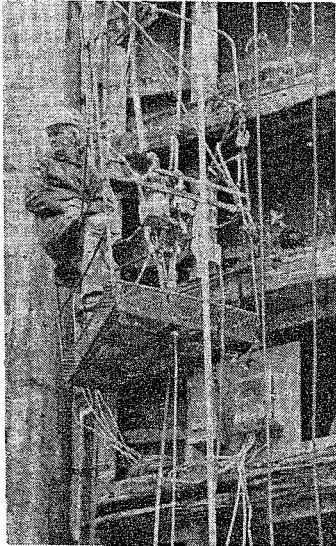
VOL 8, NO. 3

INFORMATION EXCHANGE BULLETIN

AUG 1991

US Army Corps
of Engineers

LIBRARY
USE ONLY



Workers, dressed in safety gear, carry a bucket of molten zinc with a temperature between 850 and 1,100 °F to the work site at Bankhead Lock, AL.

Zinc Backing Material Expected to Extend Service Life of Bankhead Miter Gates

by
Elke Briuer

US Army Engineer Waterways Experiment Station



Rehabilitation of lock gates can be costly to the shipping industry because of lock downtime. To cut future downtime, and thus costs, it is critical to select repair materials that have a long life expectancy. Just as significant are factors that allow these materials to be applied quickly, under conditions that are safe to the workers and the environment.

During recent lock-rehabilitation work in Alabama, material used to back the miter gates is long-wearing and safe to use. This material is zinc.

Lock gates traditionally were backed with lead. As locks were built bigger and with higher lifts, the softness of lead became a problem. The larger gates placed an increased load on the backing material during

lock operation. As a consequence, deformation of the lead, and with this misalignment of the gates, resulted. Today, new environmental and safety regulations forbid the use of lead for backing of lock gates.

During the 1970s, epoxy appeared to be the next generation of reliable material for the backing of lock gates. However, there have been instances where epoxy backing has failed within a few years of placement. The causes of failure, although investigated, have not always been determined. This has led to some doubt about the reliability of epoxy as a backing material.

Zinc as a backing material appears to ensure a long-lasting alignment of lock gates. In addition, the zinc meets OSHA and other



environmental requirements and avoids the uncertainty of reliability that is inherent with the use of various epoxies.

FIELD APPLICATION BACKGROUND

The US Army Corps of Engineers Tuscaloosa Area Office maintains its own navigation structures located in Alabama, along the Tombigbee, Black Warrior, and Alabama Rivers. Central to this work is a fully equipped and staffed repair facility. During June and July 1991, miter gates at Holt and Bankhead Locks and Dams received new contact blocks, mostly made of stainless steel, backed with zinc for durability.

The rehabilitated locks are located on the Black Warrior River, with the upper lock, Bankhead, situated approximately 30 river miles and 45 highway miles north of Tuscaloosa, AL. Engineers from the Tuscaloosa Area Office conducted the work with in-house labor and expertise. L. E. Bridges, assistant area engineer at Tuscaloosa, directed the work. A planned and coordinated, 21-day closure of both locks began June 19, 1991. The locks reopened July 10. The snagboat ROS under Captain Jerry R. Sellers supported the operation, lending both crew and crane to the project.

Bankhead Lock and Dam was built in 1914. Originally a fixed-crest structure, the dam was raised with the addition of gates to the dam in 1939.

When Bankhead received a new lock in 1975, the old lock was left in place. A newly-dug channel provides access to the larger lock, which has a 69-ft lift. The lower gates are 85 ft tall.

Originally, the miter gates of the new lock were backed with epoxy, since lead would have been subject to deformation and may have squeezed out of the high lift lock. In 1983, the epoxy backing began to fail. The old epoxy was removed and the gates were backed with new epoxy, which performed satisfactorily. In fact, the epoxy chipped from the gates during the 1991 lock rehabilitation was still good, according to Bridges.

BACKING MITER GATES WITH ZINC

Contract specifications for new lock construction offers the options of either using epoxy or zinc for the backing of the gates. Bridges pointed out that epoxy is easier to handle and safer to use, but in his view the Tuscaloosa repair facility has had better quality repairs when using zinc.

Since the area office owns two melting furnaces and has personnel with previous experience in handling and applying zinc backing material, zinc was selected to back the miter gates, once the decision was made to perform the work in-house. The furnaces are standard, gas-fired smelt-

ing furnaces, available from dealers that equip commercial industry.

Zinc comes in 50-lb ingots. For handling ease during the Bankhead rehabilitation, the ingots were cut in half and stacked in baskets near the furnaces (Fig. 1). The furnace crew, as well as anyone else working near the molten zinc, wore safety helmets and shields, foundry gloves and shin covers, and fire-retardant work coats. Zinc bars were lifted with thongs and placed into the furnace. As the bars melted, more zinc was added. The furnace was gas fired until the molten metal reached the desired temperature of 1,100 °F.

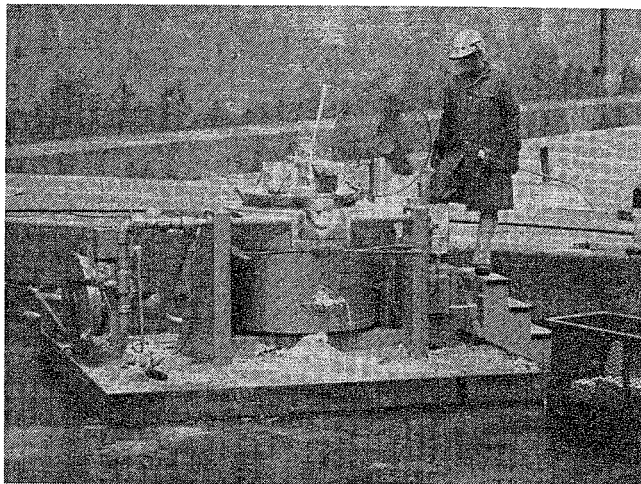


Figure 1. Furnace used to melt zinc in Bankhead lock rehabilitation. Zinc ingots are stacked in basket at lower right. Impurities skimmed off molten zinc are piled under furnace spout.

At that time, the tub was tilted to allow the molten zinc to flow into a bucket. The bucket rested on a carrying frame.

Zinc ingots generally contain 2 percent impurities that are released as the zinc is melted. The impurities float on top of the molten zinc and can easily be removed. At Bankhead, while two crew members stood ready to carry the zinc to the work site, another worker skimmed the impurities from the top of the bucket contents immediately after the zinc was poured from the furnace. After each pouring, more zinc bars were added to the tub to keep the level of the furnace contents constant.

At the work site, the bucket with the molten zinc was attached to a rope (Fig. 2), hoisted by a work crew with the help of a pulley assembly to the basket supporting the worker (see front page, top side photo) who poured the zinc. The worker used a stainless-steel funnel to pour the molten zinc between the steel block and the gate's end plate (Fig. 3). The funnel was custom made for the job at Bankhead.

The application of the zinc took place after the steel contact blocks were attached and adjusted with push-and-pull bolts. At the lower Bankhead gates, the bottom 22 ft of the blocks are stainless steel. The blocks on the upper gates are all stainless, necessary due to submerged conditions.

Although newer locks often have adjustable wall blocks, those at Bankhead are welded in place and did not need backing. The lower gates at Bankhead were receiving zinc backing behind the quoin blocks on July 9, 1991. (Note: quoin block is the proper engineering term for contact blocks on the wall-end of the gates.)

To prevent the zinc from solidifying too quickly, the blocks were preheated with electric blankets prior to pour-

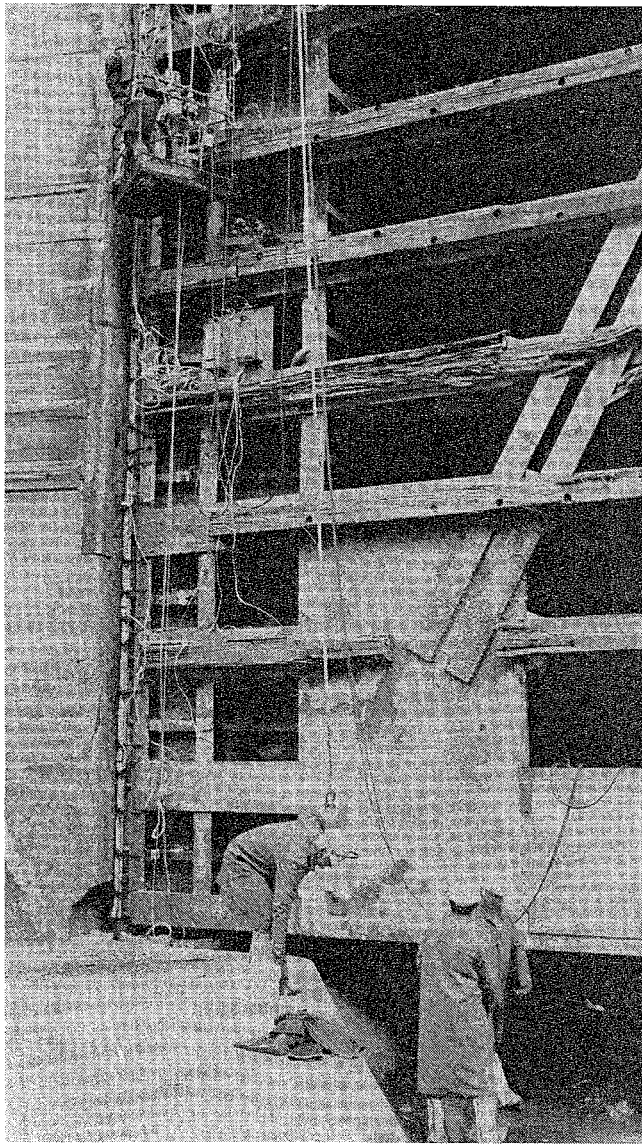


Figure 2. A worker steadies the bucket, filled with molten zinc, before the hoist crew pulls it up to the pourer. Clearly visible are blankets strapped to the stainless steel block, plugged into electrical supply visible underneath the work cage.

ing the zinc (Fig. 4). Coupled with the initial high temperature of the zinc, the heated steel block prevented cooling the zinc below its 850 °F melting point during the handling and application processes. This procedure is vital since premature solidifying of the zinc could result in voids in the backing.

The zinc was poured into staggered pour holes which were spaced approximately 4 ft apart in the end plate. On the backside of the gate, another worker unplugged alternating holes for quality control checks, some time after the temperature of the steel block rose, indicating the hot zinc had filled the void between the stainless-steel block and the frame that holds the block to the gate.

Bridges said, "The workers do this until they reach the top of the gates. Under ideal conditions, they can pour 170 ft in 8 hr. You cannot pour in the rain."

Bridges also said, "We hope that this job will last at least 25 years. Our dewatering and inspection schedule is 6 to

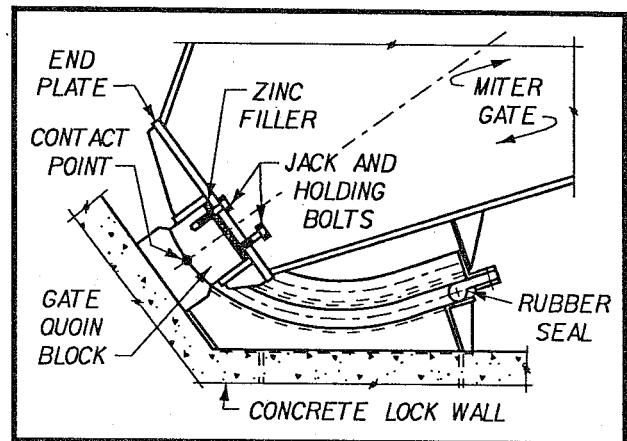


Figure 3. Schematic of a quoin showing push-pull bolts and area to be filled with zinc.



Figure 4. Close-up of a pour hole on right miter gate at Bankhead lock. Blanket heating the steel block is also visible.

8 years for high-lift and 10 years for low-lift locks. At that time, we will know how the zinc is performing.”

During the rehabilitation work, representatives from the Panama Canal visited the Tuscaloosa Area Office to gather information on the process of zinc-backed gates. Although legally lead may still be used in Panama, ideas for better and safer materials appeal to engineering professionals, who will be backing lock gates of the Panama Canal within a few years.

For more information, contact L. E. Bridges at (205) 752-3571.



Elke Briuer, Information Technology Laboratory, is a technology transfer specialist at the US Army Engineer Waterways Experiment Station. She received her B.A. degree from the University of Maryland and is a Master's candidate in mass communication at Mississippi College. She is a graduate of the Army's Public Affairs Advanced Course.

Coastal Structure Acoustic Raster Scanner (CSARS) System for Underwater Inspection



by

Jonathan W. Lott

US Army Engineer Waterways Experiment Station

The underwater part of a coastal structure often sustains more damage than the part above water, yet it is more difficult to inspect. Scour and toe damage, common for coastal structures such as breakwaters and jetties, can progress rapidly but go undetected from the surface until a collapse occurs. Waves, currents, and limited underwater visibility (normal around coastal structures) make diver and side-scan sonar surveys difficult. The resulting data are often sketchy, distorted, and qualitative.

NEW INSPECTION TOOL

A new tool for underwater inspection of coastal structures has been developed as a prototype system. The Coastal Structure Acoustic Raster Scanner (CSARS) system has been developed at the Prototype Measurement and Analysis Branch (PMAB) of the Coastal Engineering Research Center (CERC) under Gary L. Howell's leadership. CSARS was designed to be an advancement over existing technology for inspection of irregular, rubble-mound coastal structures. CSARS seeks to meet the need for a tool giving objective, detailed, and quantitative definition of underwater shape of coastal structures.

CSARS is a type of narrow-beam scanning sonar, which obtains range data through acoustic (sound energy) travel time, like a fathometer. The system consists of a bottom-deployed, pointable acoustic transducer with driving motors and attitude sensors, connected to a topside controlling computer by an umbilical cable. The bottom-sitting

tripod transducer platform allows controlled positioning of the scanner relative to the structure. The heavily weighted tripod rests firmly on the sea floor while the transducer is scanning. Hence, CSARS avoids the range errors frequently encountered when boat-mounted or towed acoustic systems are used.

In Figure 1, the underwater unit can be seen atop the bottom-sitting tripod, with the shipboard unit at lower right.

The shipboard unit consists of an IBM-compatible PC-XT with a keyboard and monitor for the operator interface and includes an analog-to-digital (A/D) converter card, a digital input/output/timer card, and a custom interface card. The computer allows operator control of scanning through a menu system.

The round transducer head and tilt motor are seen at the top of Figure 1. The head transmits pulses of acoustic energy in a very narrow conical beam pattern ("pencil beam") towards the structure along a straight ray path. The range to the target reflector (the structure) is determined from the elapsed time until the return signal (echo) is detected. The relatively low acoustic frequency of 300KHz results in a relatively long-ranging capability and allows ample structure-to-transducer standoff distance (typically 100 to 300 ft).

In addition to the transducer and the associated pan and tilt mechanisms used for precise, stepwise pointing of the scanning head, the underwater unit includes a compass and

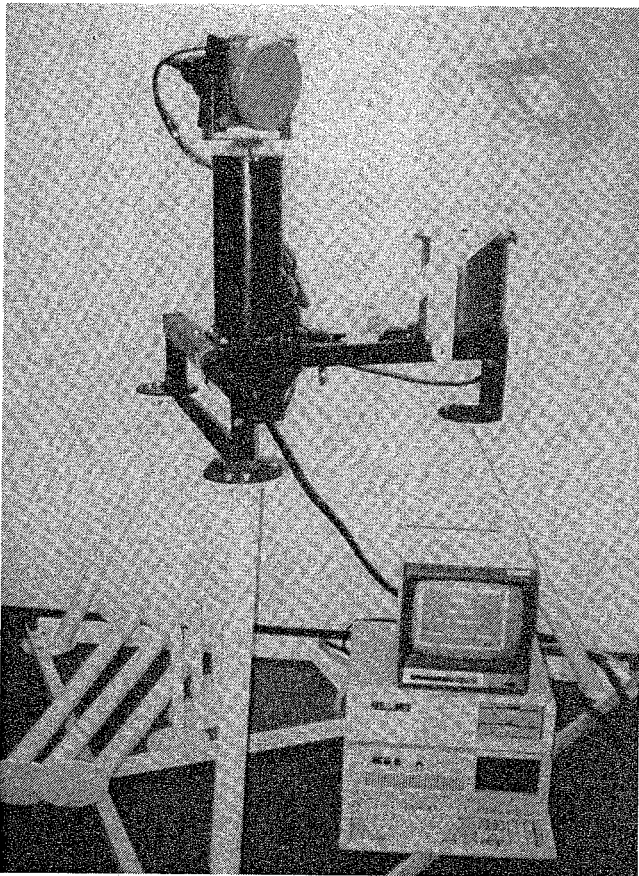


Figure 1. Coastal Structure Acoustic Raster Scanner (CSARS) System

inclinometer (measures tilt from vertical) and a pressure sensor to provide water-depth readings. The short, dark cylinder that can be seen at upper right of Figure 1 contains the digital compass. Bolting on extension legs and spikes (shown at lower left of Fig. 1) allows the transducer head to be raised farther above the sea bottom.

OPERATING CSARS

Figure 2 illustrates the operating concept of the CSARS, showing the three-dimensional "scan volume," within which range data are collected. The transducer is located at the origin of coordinates. CSARS collects range data by scanning this operator-specified region point-by-point along horizontal lines similarly to the way a television screen image is built up by the moving electron beam inside a cathode ray tube. This type of operation is called raster scanning. Each range value thus obtained corresponds to a "cell" or "bin" of the spherical raster (matrix). Good ranges (strong returns) may not be obtained for all bins.

Lack of data for portions of the scanned structure can be caused by shadowing effects or by oblique orientation (relative to the incident beam) of strongly reflective surfaces. Unlike side-scan sonar, CSARS does not store the

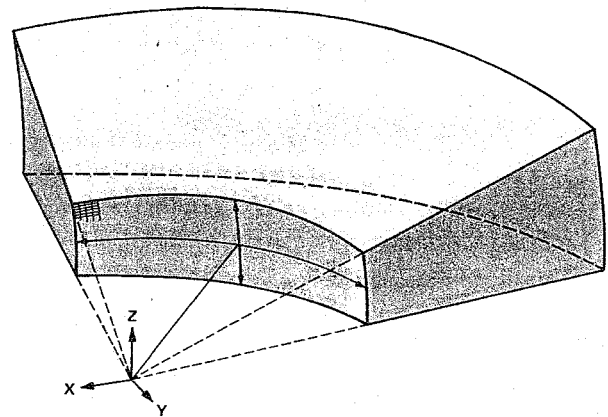


Figure 2. Scan volume diagram.

intensity of the return echoes and, therefore, cannot distinguish between reflecting materials on that basis.

Field operation involves lowering the tripod to the sea floor from a boat fitted with a suitable boom or A-frame. Diver support is not needed if entanglement of the tripod or umbilical can be avoided. Field operation is less limited by environmental conditions than other underwater inspection methods and is mostly controlled by operating limits of the deployment vessel. Deployment is envisioned as a series of set-downs of the tripod at points spaced along the coastal structure, at some safe standoff distance from the toe. Spacing and standoff distance depend on the extent of overlapping coverage desired and the geometry of each set-down's operator-specified scan volume, as well as the range capability of the system, resolution required, and shape of the structure itself. To date, field tests have not taken advantage of the possibility of merging overlapping scan data sets. To do so will require accurate knowledge of transducer positions or use of matching techniques analogous to the use of ground control in stereoscopic aerial photography.

In order to provide maximum flexibility and operator control, most of the system-operating characteristics are programmable. Operation of the instrument is controlled through the shipboard computer program, providing the man-machine interface, real-time scan monitoring, and onsite post processing and graphical display. The custom software is written in PASCAL.

SPECIAL FEATURES

After deployment, the system automatically determines the local bottom slope; that is, it measures the degree and direction of tilt of the tripod with respect to vertical and to magnetic north. These pan and tilt values (spherical coordinates) are then converted to Cartesian coordinates, whereby the transducer head is at the origin, the X axis is aligned east-west, the Y axis is aligned north-south, and the

Z axis is vertical. Positive values for x-y-z represent distances east, north, and up from the transducer head, respectively.

Automatic scanning proceeds according to specifications selected through the software menu. The operator defines the scan volume (shown as the shaded region in Figure 2) by specifying a central ray direction (azimuth and inclination) in reference to magnetic north and the horizontal plane, horizontal and vertical excursions (in degrees of arc), and minimum and maximum range limits (radial distances). Azimuth values are specified in degrees clockwise from north; inclination values are in degrees up from horizontal. Bin (cell) dimensions are determined by step-size increments in horizontal and vertical directions, also specified in degrees of arc.

Resulting digital data sets can be treated like any other spot elevation data, allowing for contouring, profiles, volume calculations, and 3-D displays. One of the features of side-scan sonar that make it useful is its image output format, which makes human interpretation easier; CSARS data can also be used to produce a variety of image output forms.

FIELD APPLICATIONS

The system has been refined following field tests at several sites and currently can accurately estimate the slope and show the general shape of a structure face. In-water trials of evolving versions of the prototype CSARS system have been conducted in several man-made tanks, in a lake, in the Atlantic Ocean near Wilmington, NC, at Cleveland Harbor on Lake Erie, and at Crescent City, CA. CSARS data proved useful as a complement to side-scan sonar imagery in making decisions about the repair of the Crescent City Breakwater.

At Crescent City, a 35-ft fishing vessel was fitted with a boom/winch deployment system assembled onsite. One of the scan volumes covered the frequently damaged transition area between stone armor units and concrete dolos armor ("Ski's Hole"). Figure 3 shows a view from the deployment vessel of the part of the breakwater being scanned. In Figure 3, the lifting apparatus and cable leading to the bottom unit can be seen, as well as a prism cluster (upper right) used with a total-station survey instrument located on the breakwater at the center of the photo. Figure 4 shows a side-scan sonar image of the area of interest (from a different date). The approximate location of the CSARS scan volume is shown overlaid on the side-scan image, in a plan view.

Figure 5 shows a plan view of the scan volume and collected data points (good ranges). The central ray for the scan volume has an azimuth of 40° magnetic and an inclination of zero. Excursions were 40° vertical and 90° horizontal. Minimum and maximum ranges were 10 and 200 ft, respectively. The step size between bins was the



Figure 3. View of Crescent City breakwater, "Ski's Hole" site, from deployment vessel.

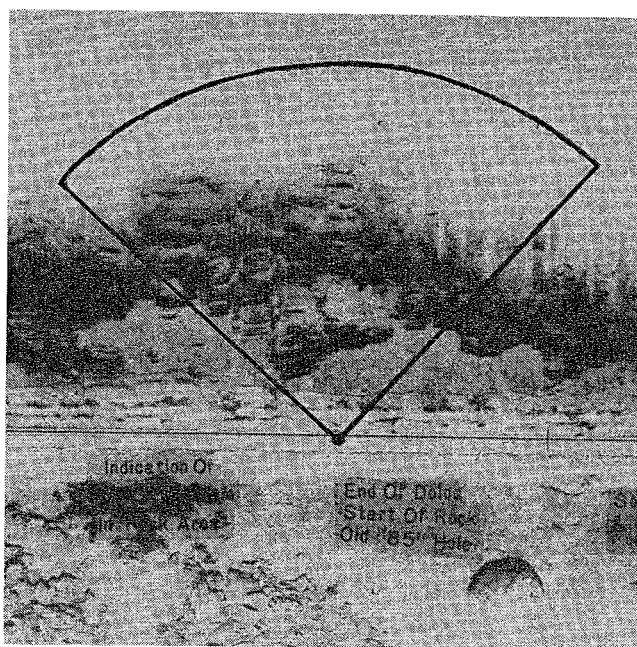


Figure 4. Side-scan sonar image of Ski's Hole site with scan volume position, obtained by William (Ski) M. Kucharski.

minimum possible (0.45°), resulting in a data set of 5,114 points. The scanning process took about 40 minutes. Seas were unusually calm during the field operation.

Figures 6 and 7 show plots produced from unfiltered data at the "Ski's Hole" site. The stacked contour plot of Figure 6 was created after the data were interpolated onto a regularly spaced 1-ft grid in the horizontal plane with a commercial PC software package with a kriging algorithm. The view is from a position above and behind the transducer position (located at coordinates 0,0,0) looking towards the breakwater, as it might be seen from aboard the deployment vessel if the water were transparent. A flat, horizontal surface is plotted in areas where data points are spread apart too far from one another horizontally. The flat areas are at an elevation corresponding to the lowest point

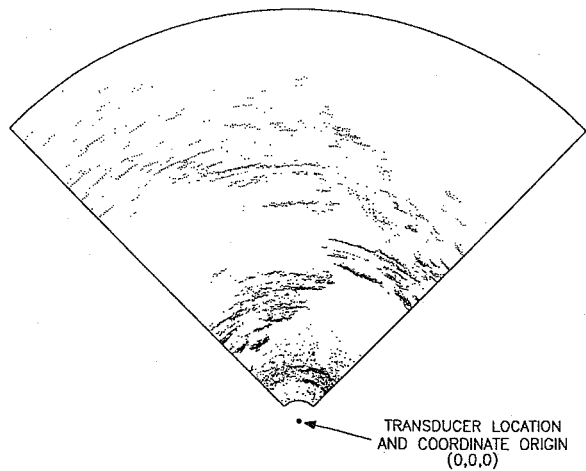


Figure 5. Scan volume and collected data points for "Ski's Hole" site.

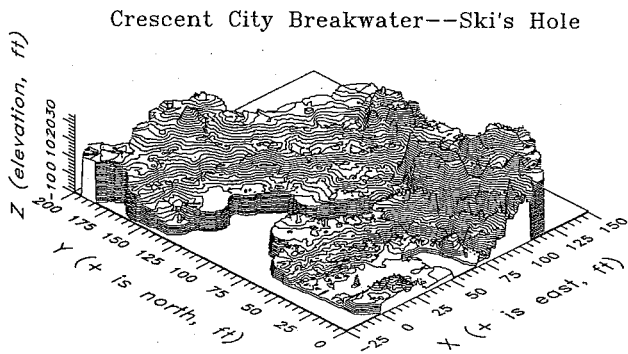


Figure 6. Stacked contour plot of a surface created from unfiltered data of "Ski's Hole" site.

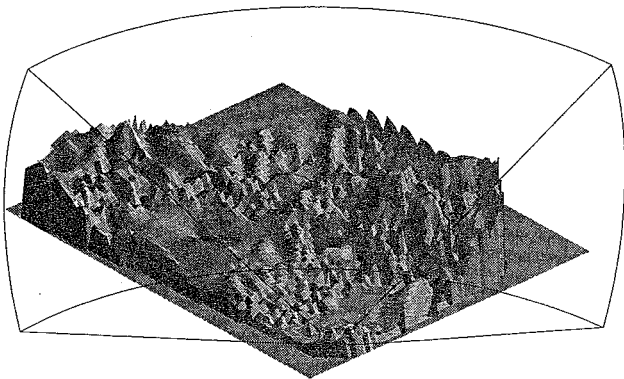


Figure 7. Shaded plot of a surface created from unfiltered data of "Ski's Hole" site.

in the data set, which is about 10 ft below the transducer elevation. Note that in addition to the stacked contour plot (1-ft contours in Figure 6), a conventional contour drawing can easily be produced. Figure 7 shows a shaded plot of a surface created from the same data set with an inverse distance gridding algorithm with a 2-ft grid size. Figure 7 was created with the use of three other PC software packages. The surface in Figure 7 shows a greater amount of bridging across data voids than that of Figure 6. The viewing position in Figure 7 is the same as that of Figure 6; the outline of the scan volume (dark lines) is also shown. In Figure 7, the flat, horizontal part of the surface is at zero elevation. Figures 6 and 7 seem to confirm the features seen in the side-scan sonar image, in spite of shadowing-related gaps in the data set. The advantage of the CSARS data set is that measurements such as slopes, lengths, areas, and volumes can be obtained relatively easily and reliably, whereas the side-scan image is not scalable. Even automatic-correcting side-scan sonars are unable to provide undistorted plan images when the sea bottom slopes in any direction other than the along-track direction. Also, wave-induced towfish motions and curving tow tracks introduce uncorrectable scale distortions.

CURRENT DEVELOPMENTS

Since the Crescent City operation, a rapid surface display capability has been incorporated so that immediate review of scan data can take place on the deployment vessel and subsequent scans can be planned accordingly.

The current CSARS is best suited to inspection of steeply sloped structures, since in a bottom-sitting configuration, parts of the structure may be obscured from the transducer's line of sight by higher foreground features. In field tests to date, CSARS has not been able to resolve individual armor units or to distinguish concrete armor units (dolosse) from armor stone. With the current system configuration and within the design operating range, minimum possible spacing between data points (with no gaps due to bad ranges or shadowing) is on the order of 2 to 3 ft. Even without any gaps in the data set (an unlikely situation), it is unrealistic to expect to be able to distinguish individual armor units with the current system.

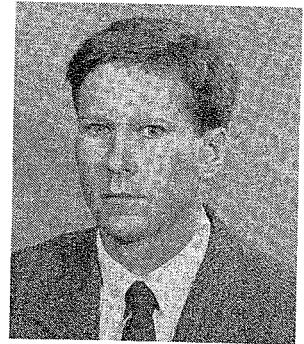
Anticipated future improvements include incorporation of accurate absolute positioning and more advanced postprocessing of the data.

These improvements should permit merging of overlapping scan data sets, more detailed and reliable definition of structure shape, and determination of changes in shape over time through repeated surveys. It is believed that overlapping scan coverage may be a key to improved resolution needed to distinguish between armor units. Storage of return signal intensity, which would help distinguish between different target materials, may be implemented if feasible.

Efforts will be directed toward providing compatibility of CSARS digital data sets with computer-based data management tools now becoming available throughout the Corps (such as Geographic Information Systems). The CSARS output imagery will be improved for easier interpretation. Improvements to the system to make field operations more efficient are also planned.

For more information contact Jon Lott, (601) 634-4268.

Jonathan W. Lott is a hydraulic engineer in the CERC Prototype Measurement and Analysis Branch, Coastal Engineering Research Center, US Army Engineer Waterways Experiment Station. He received his B.S. degree in civil engineering at the University of Maryland and his M.S. degree in coastal engineering at the University of Florida. He assisted in the REMR-I work



unit "Evaluation of Damage to Underwater Portions of Coastal Structures" and is Principal Investigator of the REMR-II work unit "Quantitative Imaging and Inspection of Underwater Portions of Coastal Structures," which includes continued development of CSARS among its objectives.

The Potential for Cracking of Silica-Fume Concrete



by

James E. McDonald

US Army Engineer Waterways Experiment Station

Laboratory tests at US Army Engineer Waterways Experiment Station in the early 1980s showed that the addition of silica fume and high-range water-reducing admixture to a concrete mixture greatly increases compressive strength, which in turn increases abrasion-erosion resistance. As a result of these tests, silica-fume concrete was used to repair abrasion-erosion damage in the stilling basin at Kinzua Dam, PA, and in the concrete lining of the low-flow channel, Los Angeles River. In each repair there was some cracking, which was ultimately attributed to restraint of volume changes resulting from thermal contraction and, possibly, autogenous shrinkage.

Recent inspections indicate the cracking has not significantly reduced the abrasion-erosion resistance of the concrete. However, such cracking could limit the use of silica-fume concrete in other repair and rehabilitation applications. Consequently, a laboratory study was conducted to determine those properties of silica-fume concrete that might affect cracking and to develop guidance on how to avoid or minimize these problems in future repair projects.

SILICA FUME TEST SPECIMENS

Concrete materials and mixture proportions similar to those used in the Kinzua Dam repair were used to cast all test specimens. The concrete mixture was proportioned

with 3/4-in. nominal maximum size aggregate for 12,500-psi compressive strength at 28 days. The water-to-cement-plus-silica fume ratio was 0.28. Slump and air content of the freshly mixed concrete averaged 9-1/4 in. and 2.2 percent, respectively.

TEST RESULTS

Detailed testing procedures and results have been reported (McDonald 1991). Results of these tests, summarized herein, were compared with the results of tests on concretes without silica fume used on recent Corps projects.

Compressive strengths of the silica-fume concrete ranged from 6,080 psi at 1 day to 14,910 psi at 1 year. The 28-day compressive strength (14,280 psi) was 96 percent of the strength at 1 year. The compressive strength of comparable concrete without silica fume and a high-range water-reducing admixture was 5,710 psi at 28 days.

Splitting tensile strengths ranged from 500 psi at 1 day to a maximum of 1,015 psi at 90 days. Overall, tensile strengths averaged approximately 7 percent of comparable compressive strengths. The normally accepted value for conventional concrete is 10 percent.

The modulus of elasticity increased with age, ranging from 4.1×10^6 psi at 1 day to 7.0×10^6 psi at 1 year. These

measured values for modulus of elasticity are essentially the same as the values calculated according to ACI 318 (1988). Overall, the average difference in actual and calculated values of modulus of elasticity was less than 6 percent. Poisson's ratio at the various test ages was essentially constant, ranging from 0.21 to 0.24.

Uniaxial creep tests were conducted on 6- by 16-in. cylindrical concrete specimens, each containing an embedded Carlson strain meter. Specimens were subjected to a sustained load of 25 percent of the ultimate compressive strength at the time of testing. Unloaded specimens subjected to the same environment were used as controls to determine volume changes under static temperature and moisture conditions.

Creep strains were obtained by subtracting the elastic strain from the total strains for each specimen and correcting this result for the appropriate volume change. Specific creep was calculated by dividing the average creep strains by the appropriate sustained load. A curve-of-best-fit based on a least-squares analysis was then computed for specific creep strains at each loading age. Specific creep strains after 1 year under load were 0.371, 0.243, and 0.176 millionths/psi for loading ages of 1, 3, and 7 days, respectively. These results appear to agree with previous reports that creep of silica-fume concrete is 10 to 20 percent less than that of comparable conventional concrete.

Drying shrinkage of silica-fume concrete was determined from strain measurements on the unloaded control specimens in the creep tests. After 1-year exposure to a temperature of 73 °F and 50 percent relative humidity, the drying shrinkage was 400, 398, and 343 millionths for tests initiated at 1, 3, and 7 days, respectively. These test results are in general agreement with previous reports that the drying shrinkage of silica-fume concrete is lower than that of comparable conventional concrete.

Periodic strain measurements on four test specimens continuously stored in a moist curing room were used to determine the volume change of silica-fume concrete in the absence of drying. Strain and temperature measurements corresponding to the time of setting were used as the zero point for calculating the autogenous shrinkage. Average results of the volume-change tests and the drying-shrinkage tests initiated at 1 day (Fig. 1) followed a similar trend, increasing shrinkage at a decreasing rate, for approximately the first 150 days. Beyond this time, all volume-change specimens exhibited expansion, reducing the net shrinkage to an average of 31 millionths at the end of the test period. Limited measurements by Saucier (1984) on 3-in. expansion bars stored in water exhibited this same trend on an accelerated time scale. In these tests, concrete with and without silica fume exhibited autogenous shrinkage to 28 days and expansion beyond this age.

Average results of the volume-change tests at early ages exhibit a rapid shrinkage of about 60 millionths within the

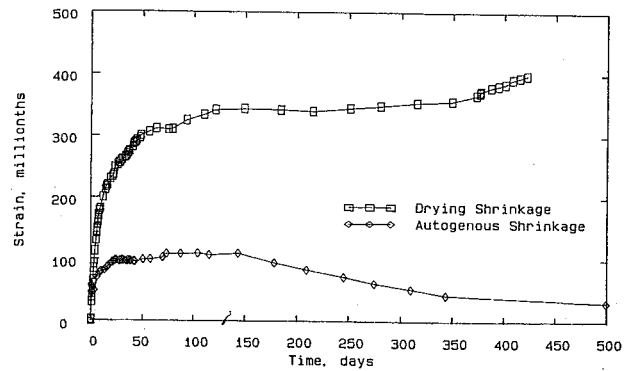


Figure 1. Average results of drying shrinkage tests initiated at 1 day and autogenous shrinkage tests

first 24 hours followed by a more gradual increase in shrinkage to approximately 80 millionths at 10 days. Similar results were reported by Paillere et al (1989), who noted that whereas conventional concrete shrinks very slowly after the usual stage of hydration swelling, silica-fume concrete exhibited no swelling stage and shrinkage was immediate. This high autogenous shrinkage is attributed to self-desiccation resulting from the hydration of the cement at a very low water-cement ratio, with or without silica fume.

The restrained volume-change of silica-fume concrete was determined by periodic length-change measurements on expansion bar specimens. Following demolding and initial length measurements at 1 day, two specimens each were continuously stored in (a) plastic bags in air, (b) moist curing room, and (c) lime-saturated water, all at 73 °F.

In each environment, shrinkage strains of the restrained specimens were slower to develop than those of the unrestrained volume-change specimens at comparable ages (Fig. 2). Specimens stored in the moist curing room and lime-saturated water expanded to day 5 and then began to shrink. At the end of the test, these specimens exhibited an average shrinkage strain of 83 millionths, 15 percent less than the unrestrained specimens. The restrained specimens

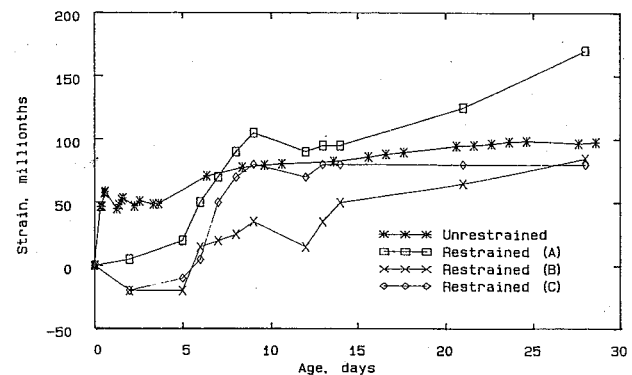


Figure 2. Autogenous volume change of unrestrained and restrained test specimens

placed in plastic bags and stored in air did not exhibit a swelling stage. With no external source of moisture, these specimens exhibited immediate and continuing shrinkage with an average strain of 170 millionths, approximately twice that of the other restrained specimens, at 28 days.

Ultimate strain capacity tests were performed on 12- by 12- by 66-in. concrete beams. Strains were measured with meters embedded parallel to the tensile and compressive faces, 1-1/2 in. from the concrete surface, and centered within the middle one-third of the span. The actual modulus of rupture for each specimen was compared to the value calculated according to ACI 318 (1988). The differences in actual and calculated values were less than 10 percent at 1 and 3 days; however, in tests beyond 3 days, the actual modulus of rupture exceeded the calculated by an average of 23 percent.

Strains measured at the strain meters were extrapolated to the surface fibers of the specimens, assuming a linear strain distribution. Strain capacities were high and generally increased with age, ranging from 124 millionths at 1 day to 223 millionths at 90 days. Both the tensile stress and strain capacities of silica-fume concrete averaged about 2-1/2 to 3 times higher than that of conventional concrete used in recently constructed Corps projects (Fig. 3).

The adiabatic-temperature-rise test had to be terminated prematurely because of equipment failure. The results obtained indicate a temperature rise for silica-fume concrete of 97.1 °F after approximately 8-1/2 days. This significantly higher temperature rise, compared with that for conventional concrete (Fig. 4), is primarily attributed to the increased cement content of the silica-fume concrete. If the test had been completed, it is expected that a temperature rise of at least 100 °F would have been recorded, a rise about 10 percent higher than predicted for conventional concrete with the same cement content.

The coefficient of thermal expansion of the silica-fume concrete was 6.7 millionths/°F. This value is similar to the values recently determined for conventional concrete used on Corps projects.

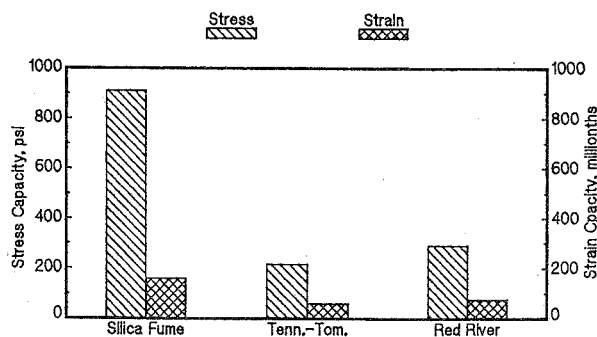


Figure 3. Tensile stress and strain capacities of silica-fume concrete compared with that of conventional concrete

Abrasion-erosion testing of three specimens was initiated at 28 days. This underwater test procedure subjects concrete specimens to the abrasive action of steel grinding balls. Abrasion-erosion losses of the silica-fume concrete, expressed as a percentage of original mass, averaged 2.9 percent. This loss is approximately 60 percent less than that for concrete without silica fume and a high-range water-reducing admixture (Fig. 5).

CONCLUSIONS BASED ON TEST RESULTS

The properties of silica-fume concrete that may affect cracking are compared with those properties of conventional concrete in the following:

- The significantly higher compressive strength of silica-fume concrete is not necessarily an advantage in resistance to cracking.
- The higher splitting tensile strength of silica-fume concrete should definitely be an advantage.

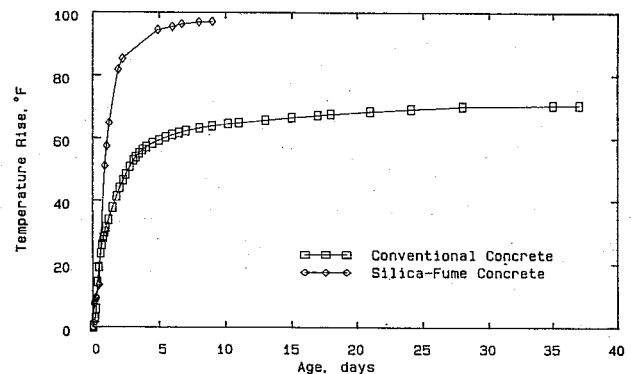


Figure 4. Adiabatic temperature rise for conventional and silica-fume concrete

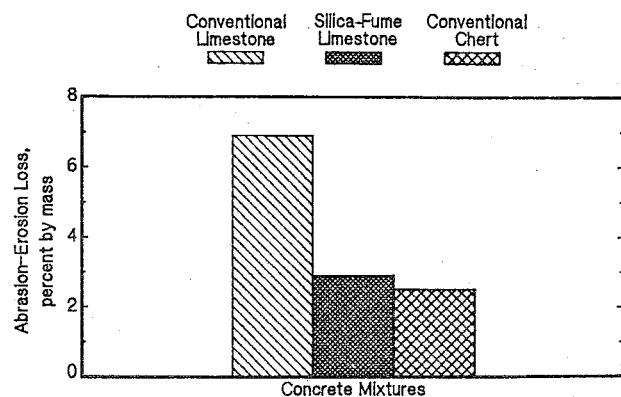


Figure 5. Abrasion-erosion resistance of limestone aggregate concrete with and without silica fume compared to conventional chert aggregate concrete

- The modulus of elasticity and poisson's ratio are comparable for the two types of concrete.
- The tensile stress and strain capacities of silica-fume concrete were 2-1/2 to 3 times higher than those of conventional concrete, a definite advantage.
- The high autogenous shrinkage of silica-fume concrete is a disadvantage.
- The lower drying shrinkage, compared to that of conventional concrete, is an advantage.
- The lower creep of silica-fume concrete may be a disadvantage in some applications.
- The higher temperature rise of the silica-fume concrete is a disadvantage.
- The coefficients of thermal expansion were comparable.

None of the properties of silica-fume concrete, with the possible exception of autogenous volume change and temperature rise, indicates that this material should be significantly more susceptible to cracking than conventional concrete. In fact, some properties, particularly tensile stress and strain capacity, indicate that silica-fume concrete should have a reduced potential for cracking.

A finite element analysis of concrete overlays placed on lock-wall surfaces (Norman et al 1989) demonstrated that restrained contraction is a predominant factor in overlay cracking. The analysis also demonstrated that an effective bond breaker at the interface between the replacement and existing concrete would eliminate cracking. Recommendations to minimize shrinkage and to install a bond breaker (Hammons et al 1989) were implemented by the Pittsburgh District in 1989 in rehabilitation of Dashields Locks. A recent examination of the project indicated that cracking of concrete placed during 1989 was significantly less than that of concrete placed during the previous construction season.

RECOMMENDATIONS

Silica fume offers potential for improving many properties of concrete; however, the very high compressive strength and resultant increased abrasion-erosion resistance are particularly beneficial in repair of hydraulic structures. Silica-fume concrete should be considered in repair of abrasion-erosion susceptible locations, particularly in those areas where locally available aggregate may not otherwise be acceptable.

The potential for cracking of restrained concrete overlays, with or without silica fume, should be recognized. Any variations in concrete materials, mixture proportions, and construction practices that will minimize shrinkage or

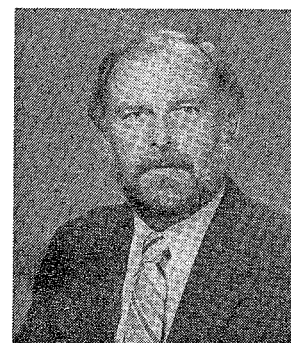
reduce concrete temperature differentials should be considered. Where structural considerations permit, a bond breaker at the interface between the replacement and existing concrete is recommended.

For further information, contact Jim McDonald at (601) 634-3230.

REFERENCES

- ACI Committee 318. 1988. "Building Code Requirements for Reinforced Concrete (ACI 318-83)," *ACI Manual of Concrete Practice*, Part 3, American Concrete Institute, Detroit, MI.
- Hammons, M. I., Garner, S. B., and Smith, D. M. 1989 (Jun). "Thermal Stress Analysis of Lock Wall, Dashields Locks, Ohio River," Technical Report SL-89-6, US Army Engineer Waterways Experiment Station, Vicksburg, MS.
- McDonald, J. E. 1991 (Mar). "Properties of Silica-Fume Concrete," Technical Report REMR-CS-32, US Army Engineer Waterways Experiment Station, Vicksburg, MS.
- Norman, C. D., Campbell, R. L., Jr., and Garner, S. 1988 (Aug). "Analysis of Concrete Cracking in Lock Wall Resurfacing," Technical Report REMR-CS-15, US Army Engineer Waterways Experiment Station, Vicksburg, MS.
- Pailiere, A. M., Buil, M., and Serrano, J. J. 1989 (Apr). "Effect of Fiber Addition on the Autogenous Shrinkage of Silica Fume Concrete," *ACI Materials Journal*, Vol 86, No. 2, American Concrete Institute, Detroit, MI.
- Saucier, K. L. 1984 (Mar). "High Strength Concrete for Peacekeeper Facilities," Miscellaneous Paper SL-84-3, US Army Engineer Waterways Experiment Station, Vicksburg, MS.

James E. McDonald is a research civil engineer in the Concrete Technology Division, Structures Laboratory, Waterways Experiment Station. He is the problem area leader for the Concrete and Steel Structures portion of REMR and the principal investigator for three REMR work units. He has been involved with various aspects of concrete research for more than 30 years. McDonald received his B.S. and M.S. degrees in civil engineering from Mississippi State University.



COVER PHOTOS:

Waiting for molten zinc, worker gets a break between pours of backing on a miter gate.

Coastal Structure Acoustic Raster Scanner (CSARS) shipboard unit.

**Current Changes to REMR
Key Personnel Roster**

Alfred D. Beitelman, CECER-EM, replaces Ashok Kumar as the Electrical and Mechanical Problem Area leader. His phone number is (217) 373-7237.

Anthony M. Kao's telephone number has changed to (217) 398-5486. Tony is the Operations Management Problem Area leader.



The REMR Bulletin is published in accordance with AR 310-2 as one of the information exchange functions of the Corps of Engineers. It is primarily intended to be a forum whereby information on repair, evaluation, maintenance, and rehabilitation work done or managed by Corps field offices can be rapidly and widely disseminated to other Corps offices, other US Government agencies, and the engineering community in general. Contribution of articles, news, reviews, notices, and other pertinent types of information are solicited from all sources and will be considered for publication so long as they are relevant to REMR activities. Special consideration will be given to reports of Corps field experience in repair and maintenance of civil works projects. In considering the application of technology described herein, the reader should note that the purpose of *The REMR Bulletin* is information exchange and not the promulgation of Corps policy; thus guidance on recommended practice in any given area should be sought through appropriate channels or in other documents. The contents of this bulletin are not to be used for advertising, or promotional purposes, nor are they to be published without proper credits. Any copyright material released to and used in *The REMR Bulletin* retains its copyright protection, and cannot be reproduced without permission of copyright holder. Citation of trade names does not constitute an official endorsement or approval of the use of such commercial products. *The REMR Bulletin* will be issued on an irregular basis as dictated by the quantity and importance of information available for dissemination. Communications are welcomed and should be made by writing the Commander and Director, US Army Engineer Waterways Experiment Station, ATTN: Elke Briuer (CEWES-SC-A), 3909 Halls Ferry Road, Vicksburg, MS 39180-6199, or calling 601-634-2587.

LARRY B. FULTON
Colonel, Corps of Engineers
Commander and Director

OFFICIAL BUSINESS
CEWES-SC-A

DEPARTMENT OF THE ARMY
WATERWAYS EXPERIMENT STATION, CORPS OF ENGINEERS
3909 HALLS FERRY ROAD
VICKSBURG, MISSISSIPPI 39180-6199

BULK RATE
U.S. POSTAGE PAID
Vicksburg, MS
Permit No. 85